IEEE Access
Multidisciplinary | Rapid Review | Open Access Journal

Received December 1, 2019, accepted December 16, 2019, date of publication December 23, 2019, date of current version January 2, 2020.

Digital Object Identifier 10.1109/ACCESS.2019.2961364

Skid-Proof Operation of Wheel Loader Based on Model Prediction and Electro-Hydraulic Proportional Control Technology

BINGWEI CAO, XINHUI LIU, WEI CHEN, KUO YANG, AND PENG TAN
School of Mechanical and Aerospace Engineering, Jilin University, Changchun 130022, China
Corresponding author: Wei Chen (chenwei_1979@126.com)

This work was supported by the National Key Research and Development Program of China under Grant 2016YFC0802904.

ABSTRACT Wheel loader shovel loading operation tests showed that when the tire slips, it not only causes waste of the engine power, but also increases the tire wear. In this paper, the regression prediction model is combined with the electro-hydraulic proportional control technology. For the first time, the method of adjusting the posture of the working device is proposed to realize the skid-proof shovel control strategy of the wheel loader. In this control strategy: (1) The electro-hydraulic proportional control technology applied to this wheel loader is introduced. (2) The load spectrum of the wheel loader is analyzed during the shovel loading operation. Moreover, combined with the drive shaft torque, pilot pressure and boom cylinder displacement, the particle swarm optimization-support vector machine (PSO-SVM) algorithm is used to complete the construction of the regression prediction model of the boom cylinder displacement. (3) A controller is designed based on the fractional-order PID control algorithm. The skid-proof control strategy is simulated and verified by constructing the joint simulation model. The corresponding program is prepared in the hydraulic system controller and the effectiveness of the control strategy and algorithm are verified by the wheel loader shovel loading operation.

INDEX TERMS Electro-hydraulic proportional control technology, PSO-SVM, regression prediction model, skid-proof shovel control strategy.

I. INTRODUCTION

Wheel loaders are commonly used for material excavation, loading and short-distance transportation in engineering construction and mining. Studies have shown that when the wheel loader shovel loading operation, it is easy to cause the wheel to slip due to the load, results in the waste of power and transitional wear of the tire [1]–[3]. Therefore, experienced drivers adjust the working device attitude of the wheel loader in real time to reduce the wheel slippage. Which is also the main content of the present study, the skid-proof operation is performed by learning the driver's operation.

Combined with related algorithms to control the skid-proof differential can achieve wheel skid-proof operation [4]–[7]. Chen *et al.* [8] studied the skid-proof control method of a four-wheel drive wheel loader. The cylinder pressure in the hydraulic limited-slip differential is controlled by the fuzzy algorithm, which realized the drive skid-proof control of the wheel loader. Fan *et al.* [9] designed a driving skid-proof control strategy based on the transmission and the engine output torque to control the cylinder pressure in the differential. The simulation results showed that the designed control strategy can effectively reduce the wheel slip rate and improve the starting acceleration in the snowy and icy road. Moreover, Zheng [10] proposed a voltage-controlled hydraulically driven differential and designed a single-chip microcomputer as the required hardware with the corresponding software to control the chip. In order to verify the skid-proof performance, a simulation based on fuzzy algorithm was carried out. The foregoing skid-proof measures should be controlled the differential by the relevant algorithm. However, the wheel loader differential studied in this paper is packaged in the transaxle so that the skid-proof control cannot be realized by controlling the differential.

The vibratory shovel can effectively reduce the working resistance of the wheel loader and reduce the energy loss. The mechanism is realized by timely destroying the compact core of the soil. Yin *et al.* [11] conducted a preliminary study on

The associate editor coordinating the review of this manuscript and approving it for publication was Salman Ahmed.

wheel loader vibrating shovel. They showed that the vibrating shovel can increase the insertion depth, reduce the insertion resistance, increase the productivity and improve economic benefits. Fan [12] used the bucket hydraulic cylinder of the wheel loader as the excitation component for the vibration insertion. He employed the accumulator as the power source and proposed the hydraulic vibration shovel loading scheme. Then he carried out experimental tests and obtained the influence of the vibration frequency and amplitude on the insertion resistance. However, the vibrating shovel needs to be modified by the original hydraulic pipeline, and adding the accumulator and the high-frequency directional valve, the mechanism of the skid-proof shovel is more complicated than the one proposed in this paper.

At this stage, there are few wheel loaders equipped with an electro-hydraulic proportional control system, so the skid-proof shovel function cannot be realized. In this paper, the wheel loader with electro-hydraulic proportional control technology is used as the carrier, and the skid-proof shovel function of the wheel loader can be realized without the hydraulic pipeline modification. It should be indicated that the electro-hydraulic proportional control technology is widely used in various fields as a bridge between modern electronic technology and high-power engineering control equipment [13], [14]. Gao *et al.* [15] established a model for the electro-hydraulic proportional control hydraulic leveling system for the heavy-duty hydraulic platform. Then they analyzed the proposed model, obtained the transfer function of the hydraulic legs. Li *et al.* [16] studied the application of the electro-hydraulic proportional control technology in the speed control system of the conveyor. They analyzed the static and dynamic response characteristics of the system. It should be indicated that the wheel loader of the present study uses electro-hydraulic proportional control technology to realize the action of the working device through the electromagnetic proportional pressure reducing valve. After learning the driver's operation through the regression prediction model, the hydraulic system controller can control the on/off of the proportional pressure reducing valve, thereby automatically adjusting the posture of the working device to achieve the skid-proof operation. In fact, the application of the electro-hydraulic proportional control technology provides a platform for realizing the skid-proof shovel operation function.

In order to realize the skid-proof shovel loading function of the wheel loader, the displacement of the boom cylinder needs to be predicted by regression. Therefore, the support vector machine (SVM) algorithm is proposed in the present study to realize the regression prediction of the cylinder displacement. SVM algorithm is based on the principle of the structural risk minimization in the statistical learning theory, which can maximize the promotion ability of learning machines. Moreover, the SVM can theoretically obtain the global optimal solution and can achieve higher accuracy with few samples for the training. In order to improve the prediction accuracy, in it intended to apply the particle swarm optimization (PSO) algorithm in the SVM model to optimize the parameters [17], [18]. In order to resolve the problem of low generalization capacity in predicting the vibration environment of the aircraft platform, Zhang *et al.* [19] combined the PSO and SVM algorithm to propose a novel predicting model. They found that the optimized SVM model can solve the conventional practical problems such as small samples, nonlinear and partial infinitesimal. Lins *et al.* [20] used the SVM in liaison with the PSO. Then tackle reliability prediction problems based on time series data of engineered components. Comparisons of the obtained results with those given by other time series techniques indicated that the PSO-SVM model is able to provide reasonable reliability predictions with comparable accuracy. However, the PSO-SVM algorithm has not been found to be used in the skid-proof shovel function of the wheel loader, which is also an innovative point of this paper.

This paper firstly proposes a skid-proof shovel loading function of the wheel loader. This function uses the electro-hydraulic proportional technology as the carrier to control the on/off of the electromagnetic proportional pressure reducing valve through the regression prediction model of the displacement of the boom cylinder, thereby changing the posture of the working device.

This manuscript is organized as follows: The analysis and research of the skid-proof shovel mechanism is presented in section 2. Then the electro-hydraulic proportional control technology is introduced in section 3. Section 4 is dedicated to the regression prediction of the boom cylinder displacement. Finally, the verification of the skid-proof shovel mechanism is presented in section 5.

II. RESEARCH ON THE SKID-PROOF SHOVEL MECHANISM

Studies show that reducing the working resistance during the shovel loading can reduce the slippage of the wheel. Therefore, the focus of the drag reduction insertion is to adjust the posture of the working device when the wheel loader is shoveling so that the wheel loader can independently assist the driver to complete shoveling operation. The following describes the mechanism of the skid-proof shovel loading of the wheel loader through the theoretical analysis.

A large part of the energy during the operation of the wheel loader is consumed during the excavation, cutting and moving of the soil, so the interaction between the bucket and the soil, the cutting mechanism and the influencing factors should be studied in detail. In the shovel loading operation, compressive deformation, shear deformation and tensile deformation of the soil generally occur [21].

With the insertion of the bucket, the soil in front of the blade is moved forward so that it undergoes compression deformations. When the soil reaches to a certain amount and moves a certain distance, a compact core is formed [22]. The principle of the compact core formation during the shovel loading is shown in Fig. 1(a). It should be indicated that the appearance of the compact core greatly increases the

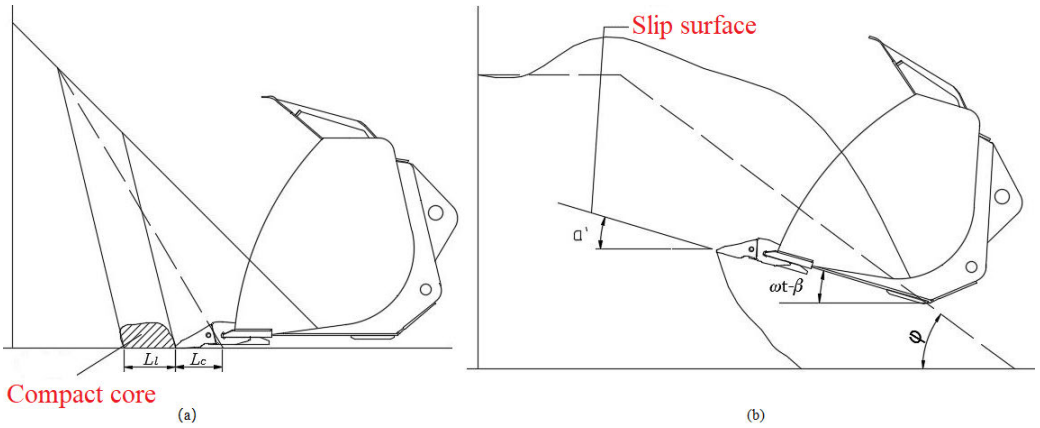

FIGURE 1. Shovel loading mechanism.

working resistance. If the traction is greater than the insertion resistance, the compact core will be destroyed and the working resistance will decrease. However, if the traction is less than the insertion resistance, it will cause the wheel to slip. Meanwhile, the posture of the working device should be adjusted to destroy the compact core and reduce the working resistance. It should be indicated that continuing the insertion continuously forms new compact cores. When the bucket is rotated, the shear resistance of the soil has been overcome. Fig. 1(b) illustrates the slip surface at a certain angle between the soil and the ground.

The length of the compact core L_l can be expressed as the following [23], [24]:

$$L_l = 1.2\frac{L_C d_a K_f K_3}{0.7 + 0.23 d_a} \tag{1}$$

where L_C and d_a are the insertion depth and the average diameter of the soil particles, respectively. Moreover, K_f and K_3 denote the bucket coefficient and the influence factor corresponding to the angle between the bucket bottom and the ground inclination, respectively.

When inserting a certain depth, the soil particles of the bucket tip are in different directions and sizes from the cutting movement [25]. Therefore, the compact core length L_l' is defined as:

$$L_l' = K_{\omega t} e^{cwt} L_l \tag{2}$$

$$K_{\omega t} = 1 + (0.45 - 0.02\alpha') \cdot 0.05\omega t$$

$$\alpha' = \frac{\ln(\omega t + 1)}{\cos \omega t} \tag{3}$$

where $K_{\omega t}$ and ω are the compact core direction coefficient and the bucket rotary angular velocity, respectively. Moreover, t and c denote the bucket swing time and the material height coefficient, respectively.

The correlation between the insertion resistance P_c and insertion depth L_C is [26]:

$$P_c = KL_C^n \tag{4}$$

Equation (4) can be approximated by the insertion resistance and the length of the compact core in the form below:

$$P_c = K' L_l^n \tag{5}$$

where K' is the influence coefficient associated with the material.

The foregoing analysis shows that the length of the compact core directly affects the insertion resistance. When the length of the compact core increases, the insertion resistance increases too. Moreover, when the compact core is destroyed and its length is shortened, the insertion resistance is expected to be reduced. Destroying of the compact core can be performed by adjusting the posture of the working device so that the tip of the bucket runs a distance and breaks the compact core. As the wheel loader advances, this operation is repeated and the compact core continues to be destroyed until the bucket is full of material.

Therefore, when the tire slippage is about to occur, if the posture of the wheel loader working device can be reasonably adjusted and the length of the compact core is destroyed in time, the engine power can be effectively utilized. The proposed skid-proof shovel mechanism is established based on the foregoing theory. The posture of the working device is adjusted by predicting the displacement of the boom cylinder. The conventional wheel loader working device is controlled by a hydraulic handle(equivalent to pressure reducing valve) that controls the output pilot pressure. Moreover, a proportional valve and related controlling devices should be added to realize the skid-proof shovel. The wheel loader uses electro-hydraulic proportional control technology to provide a platform for the implementation of these functions.

III. ELECTRO-HYDRAULIC PROPORTIONAL CONTROL TECHNOLOGY

A. CONTROL MECHANISM

The wheel loader uses the electro-hydraulic proportional control technology to control the working device operation. The electro-hydraulic proportional technology can provide a

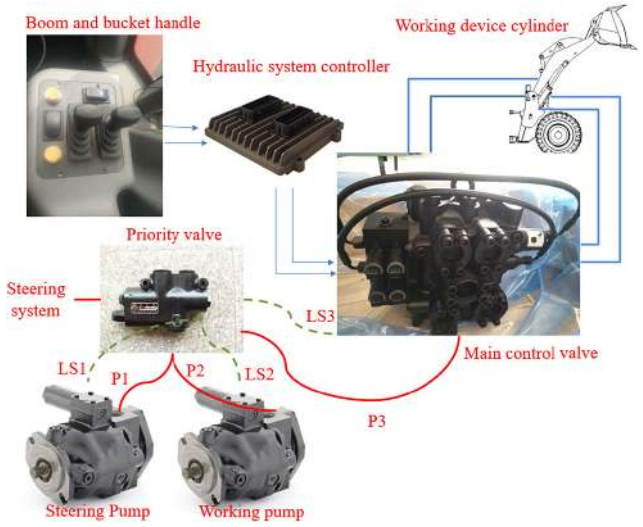

FIGURE 2. Electro-hydraulic proportional control technology.

carrier for other advanced controlling algorithms, improve the intelligence level of the wheel loader operation and reduce the fatigue of the driver. Description of the control mechanism: the handle is used as the front-end signal generator to generate the control voltage and send this voltage to the hydraulic controller. Then the hydraulic controller performs corresponding calculations in accordance with the front-end signal and outputs the current to the electromagnetic proportional pressure-reducing valve, which is converted into the pilot pressure-controlling valve, and the pair is completed.

Fig. 2 illustrates the schematic diagram of the electro-hydraulic proportional control technology of the working device(the illustration shows the control logic, not the hydraulic schematic). It is observed that the hydraulic system of the working device adopts the load-sensing dual-pump confluence technology. When the steering is not performed, the working device cylinder is supplied with the oil by two load-sensitive pumps through the main control valve.

Electrical characteristics of the handle are described as the following:

$$U = K_l \cdot \theta \tag{6}$$

where K_l and θ represent the handle scale factor and the handle action angle, respectively. It should be indicated that the handle action angle varies from $-20° \leq \theta \leq 20°$. Moreover, the output voltage varies from 0.5V to 4.5V.

When the analog voltage signal is generated by the handle, it is sent to the hydraulic system controller for processing, while the current signal is sent to the electromagnetic proportional pressure-reducing valve, where the output I is defined as the following:

$$I = K_a U \tag{7}$$

where K_a is the voltage-current gain of the controller, which is set to 0.215. The equation of motion of the proportional pressure-reducing valve spool can be expressed as:

$$M_j \frac{d^2y}{dt^2} + B_y \frac{dy}{dt} + p_2 A + K_1(y + y_0) = K_m I \tag{8}$$

where M_j, B_y and P_2 denote the spool quality, viscous damping coefficient of the spool and the outlet pressure of pressure-reducing valve, respectively. It should be indicated that the valve pressure varies from the ambient pressure to 2.5MPa ($0 \leq P_2 \leq 2.5Mpa$). Moreover, A, K_1, y_0 and K_m are the spool end face stress area, return spring stiffness, spring pre-compression and the proportional electromagnet electromagnetic force coefficient, respectively.

The main control valve is remotely controlled by the electro-hydraulic proportional valve, where this pressure-reducing valve is integrated in the main control valve. It should be indicated that the turn-on and the final currents are 300mA and 500mA, respectively. Moreover, the main control valve adopts an internal oil circuit in parallel form, which can realize the joint operation of the boom and the bucket.

B. SIMULATION MODEL

In order to understand the skid-proof shovel function, it is necessary to build a simulation model of the electro-hydraulic proportional control hydraulic system. Fig. 3 illustrates the model of the loading electro-hydraulic proportional control hydraulic system established by the AMEsim software. In the present study, the raising stage of the boom cylinder is simulated. Meanwhile, the rising position electromagnetic proportional pressure-reducing valve 1 is energized and the pilot oil acts on the main control valve 3 through the pressure-reducing valve to move the spool to the left. The hydraulic oil in the variable pump 5 is driven by the main control valve 3 to drive the boom cylinder 4 to rise. The pilot oil on the other side of the main control valve 3 spool flows back to the tank via the lowering position electromagnetic proportional pressure-reducing valve 2. When basic parameters in the simulation model are set in accordance with the sample data, the simulation is performed. It should be indicated that the simulation time is 20s. Fig. 4 shows the handle voltage, pilot pressure and boom cylinder displacement when the boom is raised.

In order to validate the skid-proof shovel function of wheel loader, the pilot proportional control system simulation model should be validated. After connecting the data acquisition instrument, the loading arm ascending test of wheel loader is carried out. Fig. 5 shows the obtained boom handle voltage, boom no-rod pilot pressure and the boom cylinder displacement.

Fig. 4 and Fig. 5 shows that with the control pressure input, the boom cylinder displacement linearly increases. At this time, the main valve control chamber pressure is 2.33Mpa and the cylinder reaches the maximum extension position of 0.978m at 15.3 s. Moreover, it is observed that the output voltage is 2.5V when the handle is in the middle position. Taking no action at this time, when the maximum

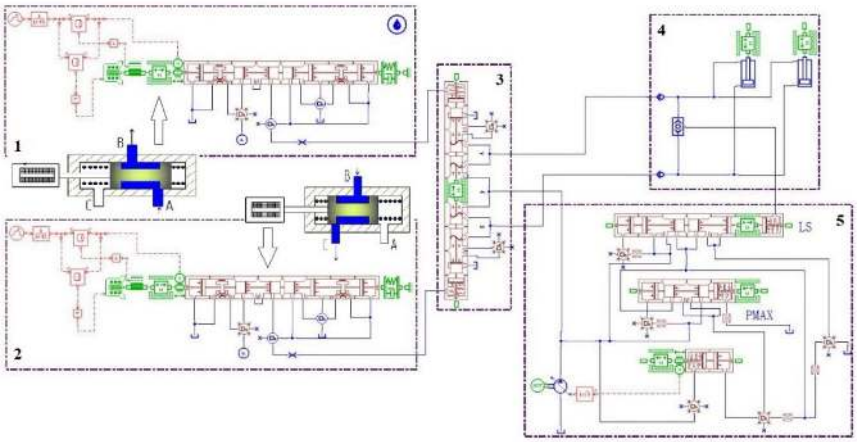

1. Ascending position electromagnetic proportional pressure reducing valve 2. Lowering position electromagnetic proportional pressure reducing valve 3. Main control valve 4. Boom cylinder 5. Variable pump

FIGURE 3. Electro-hydraulic proportional control hydraulic system model.

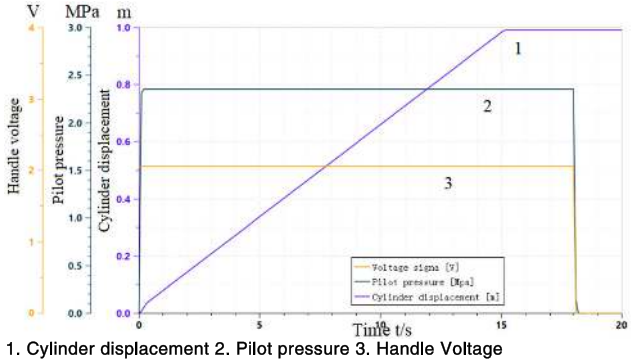

1. Cylinder displacement 2. Pilot pressure 3. Handle Voltage

FIGURE 4. Simulation curve.

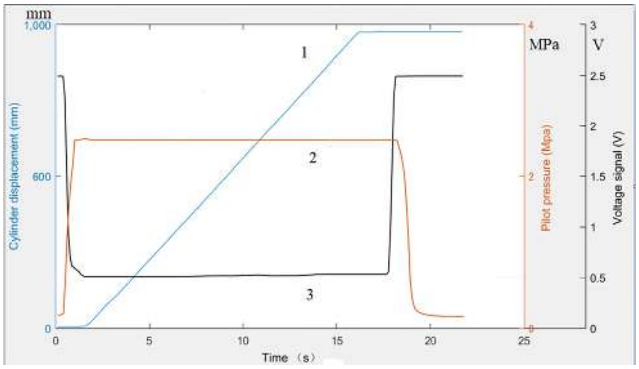

1. Cylinder displacement 2. Pilot pressure 3. Handle Voltage

FIGURE 5. Distribution of various parameters in the experiment.

opening voltage of the handle is 0.56V, the output pressure of the electromagnetic pressure-reducing valve is 2.29MPa and the piston rod displacement of the hydraulic cylinder reaches the maximum extended position at 16.2s. The test results prove the correctness of the simulation model.

The pressure curve is compared below, and the cylinder pressure curve is shown in Fig. 6. It can be seen from the figure that the change trend of the rod-free cavity pressure curve of the boom cylinder is consistent, and the maximum pressure is 25 MPa. During the simulation, the boom cylinder has been lowered to the limit position for a period of time, so the pressure will reach 25 MPa. However, the above operation was not performed during the test. The pressure curve further proves the correctness of the simulation model.

IV. DATA PREDICTION MODEL

The SVM has advantages of strong generalization ability and reasonable fitting precision and it can be used for predicting the displacement of the boom cylinder during the shovel loading operation. Moreover, the particle swarm optimization algorithm is used to optimize parameters in the SVM. Fig. 7 shows the flow of the particle swarm optimization algorithm of the optimized support vector machine for the modeling of the boom cylinder displacement. When the tire slips, the torque of the drive shaft will drop, which means that the attitude of the working device should be adjusted to destroy the compact core. The data required to complete the boom displacement prediction are the drive shaft torque, the pilot pressure, and the boom cylinder displacement.

A. SVM

SVM regression and classification are very similar in theory. The SVM regression problem is a further extension of the SVM classification application. It maps data in low-dimensional space to high-dimensional space through nonlinear mapping and in high-dimensional space to original low-dimensional space. Moreover, the nonlinear function is discriminated. Each set of data in the training sample is transformed into a high-dimensional space and data is linearly regressed in a high-dimensional space, thereby transforming the nonlinear fitting problem of the original sample into a linear regression problem of the sample in the high-dimensional space. The obtained fitting function is [27]:

$$f(x) = w \cdot \varphi(x) + b \tag{9}$$

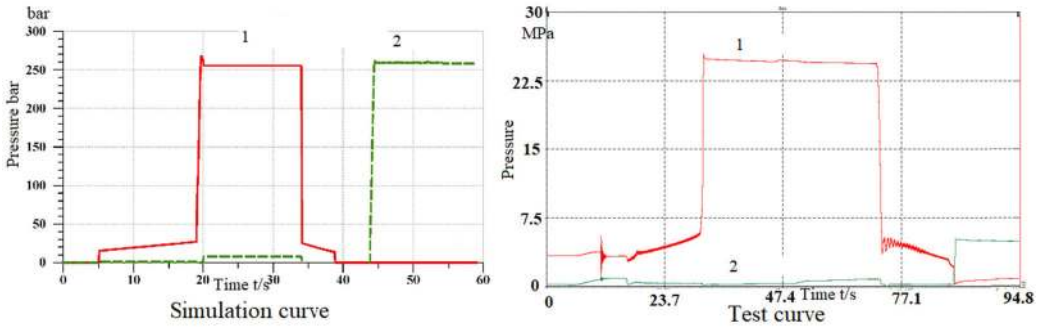

FIGURE 6. Boom cylinder pressure curve comparison.

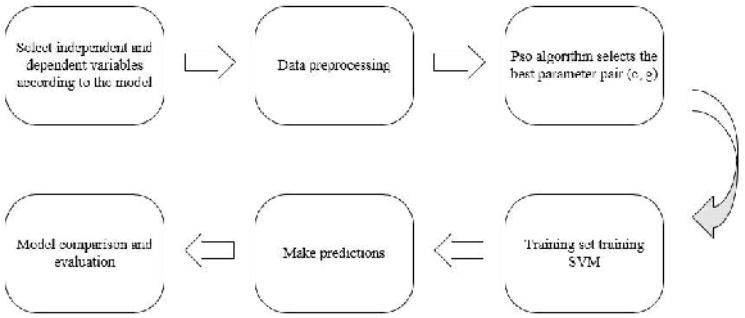

FIGURE 7. Modeling process.

where, w, x and b represent the weight vector of the sample($w \in R_n$), the input vector of the sample ($x \in R_n$) and the fitting deviation of the sample ($b \in R_n$), respectively.

$$R_{reg}(f) = c\sum_{i=1}^{n}\Gamma(f(x_i) - y_i) + \frac{1}{2}w^2 \tag{10}$$

$$\Gamma(f(x_i) - y_i) = \frac{1}{n}\begin{cases} |f(x_i) - y_i| - \varepsilon & |f(x_i) - y_i| \geq \varepsilon \\ |f(x_i) - y_i| < \varepsilon \end{cases} \tag{11}$$

where $c\sum_{i=1}^{n}\Gamma(f(x_i) - y_i)$ is the empirical error for the optimization problem and $\frac{1}{2}w^2$ is the normalization parameter for the optimization problem. Moreover, $\Gamma(\cdot)$ is the cost parameter for the optimization problem, the operation of the parameter is mainly used to compensate the normalization parameter and the empirical error, and the penalty for the optimization problem. c is the penalty factor indicating the optimization problem. The factor is such that the error of the entire training process is maintained within the normal range; ε is the parameter representing of the optimization problem loss function.

In order to reduce the error generated during the sample training process, the relaxation variable is added in the original calculation process: ξ and ξ^*, then equation (9) can be transformed into [28]:

$$\min \frac{1}{2}\omega^2 + c\sum_{i=1}^{n}(\xi + \xi^*) \tag{12}$$

$$s.t\ \xi^* \begin{cases} y_i - \omega \cdot \varphi(x) - b \leq \varepsilon + \xi \\ \omega \cdot \varphi(x) + b - y_i \leq \varepsilon + \xi \end{cases} \tag{13}$$

In order to simplify the prediction process, it is transformed into a dual problem [29], [30]:

$$\begin{cases} \max \sum_{i=1}^{n} y_i(a_i - a_i^*) - \varepsilon\sum_{i=1}^{n}(a_i + a_i^*) \\ \quad -\frac{1}{2}\sum_{i=1}^{n}\sum_{j=1}^{n}(a_i - a_i^*)(a_j - a_j^*)K(x_i, x_j) \\ s.t\ \sum_{i=1}^{n}(a_i - a_i^*) \leq a_i, a_i^* \leq c \end{cases} \tag{14}$$

where a_i and a_i^* both are used to indicate the Lagrangian multiplier added during training. The SVM model functions obtained from the abovementioned equations are as the following:

$$f(x) = \sum_{i=1}^{n}(a_i - a_i^*)K(x_i, x_j) + b \tag{15}$$

where $K(x_i, x_j)$ represents the kernel function of the SVM model.

B. PSO

The particle swarm optimization (PSO) algorithm is widely used in parameter optimization problems in fields of communication and chemical industry because of its simple structure and fast convergence [31], [32]. The velocity and position of particles depend on following equations:

$$v_{t+1} = wv_t + c_1r_1(p_t - x_t) + c_2r_2(G_t - x_t) \tag{16}$$

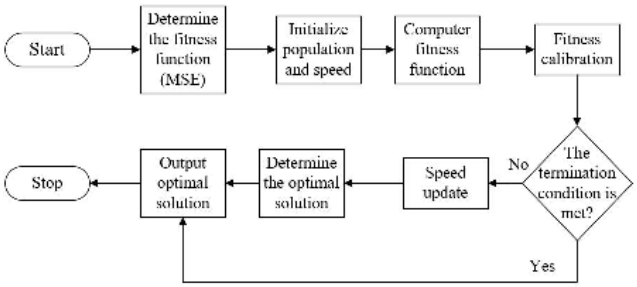

FIGURE 8. The PSO algorithm flow chart.

$$x_{t+1} = x_t + v_{t+1} \tag{17}$$

where, x, v and w represent the position of the particle, the velocity of the particle and the inertia factor, respectively. Moreover, c_1 and c_2 are the acceleration constants. r_1 and r_2 are random numbers between 0 and 1. Moreover, P_t and G_t are the optimal position searched by the particle and the optimal location currently searched for the whole particle swarm, respectively.

Fig. 8 shows the flow chart of the PSO.

The following are the steps of the PSO algorithm [33], [34].

Step1: Assign an initial value to the particle swarm, generate the random positions and velocities of all particles and determine P_t and G_t of the particle swarm.

Step2: The fitness value of each particle is compared with the fitness value of the optimal position P_t. Pick the best one as the current P_t.

Step3: The fitness value of each particle is compared with that of the G_t of the optimal position experienced by the whole particle swarm. Pick the best one as the current G_t.

Step4: Update the velocity and position of particles according to equations (16) and (17);

Step5: If it does not meet the termination condition, return to step2. Otherwise, the exit algorithm obtains the optimal solution.

C. REGRESSION PREDICTION

In the present study, the research team and a company cooperated to develop a 5-ton wheel loader prototype to carry out the wheel loader shovel test. During the test, the engine speed and torque are collected by connecting the CAN communication module. Torques of the front and rear driving shafts are monitored through wireless torque sensors. Moreover, the boom cylinder displacement, the boom pilot pressure and the boom handle voltage are obtained from appropriate data acquisition instruments. Fig. 9 shows the test connection device.

The foregoing experiment results in the load spectrum of the wheel loader during the shovel loading operation. It should be indicated that inputs of the predicted model are the drive shaft torque, boom handle voltage and the pilot pressure of the boom handle and the corresponding output is the boom cylinder displacement. Fig. 10 shows the regression prediction model for obtaining the displacement of the boom cylinder and Fig. 11 shows the error curve.

In order to verify the accuracy of the PSO-SVM regression prediction algorithm, the BP neural network is applied for the predictive analysis. Fig. 12 illustrates the obtained displacement curve of the boom cylinder from the BP neural network and Fig. 13 shows the corresponding error curve.

It is observed that the average accuracy of the prediction model is 86.41%, and the mean square error (MSE) of the predicted data in comparison to the experimental test data is 0.0289. The abovementioned comparison shows that the PSO-SVM prediction model of the transmission shaft torque has reasonable generalization ability and high forecasting accuracy.

V. SKID-PROOF SHOVEL FUNCTION VERIFICATION

In the foregoing analysis, the simulation model of the electro-hydraulic proportional control system and the regression prediction model of the boom cylinder displacement are established. In this section, it is intended to describe the skid-proof shovel function of the wheel loader working device. Fig. 14 shows the verification process for the skid-proof shovel function.

During the shovel test, the PSO-SVM regression prediction model is applied to predict the displacement of the output boom cylinder by collecting the drive shaft torque signal, the handle voltage signal and the pilot pressure signal. The boom displacement sensor, which is installed on the boom cylinder, monitors the boom displacement when the wheel loader is shoveling. Then the difference signal of the displacement is used as an input signal of the hydraulic system controller. Moreover, the controller uses a fractional-order PID control algorithm to generate a current to control the on/off of the electromagnetic proportional pressure-reducing valve, thereby controlling the movement of the boom cylinder.

The simulation of the skid-proof control strategy is carried out by establishing a joint model of the fractional-order PID control algorithm and the electro-hydraulic proportional control system.

In the present work, the Oustaloup filter is applied to approximate the fractional calculus operator. Since this operator cannot directly calculate the equation in practical applications, only the filter can be used to approximate the equation.

The approximate transfer function form of the Oustaloup discrete method can be written in the form below:

$$H(s) = \left(s/\omega_\mu\right)^\alpha, \alpha \in R^+ \tag{18}$$

Substituting s/ω_μ with $C_0\frac{1+s/\omega_b}{1+s/\omega_h}$ in a given frequency band $[\omega_A, \omega_B]$, where $(\omega_b\omega_h)^{1/2} = \omega_\mu$, $\omega_b < \omega_A$, $\omega_h > \omega_B$; $C_0 = \frac{\omega_b}{\omega_\mu} = \frac{\omega_\mu}{\omega_h}$. Based on the above alternative methods, the transfer function can be expressed as the following:

$$H(s) = \lim_{n\to\infty} \hat{H}(s) \tag{19}$$

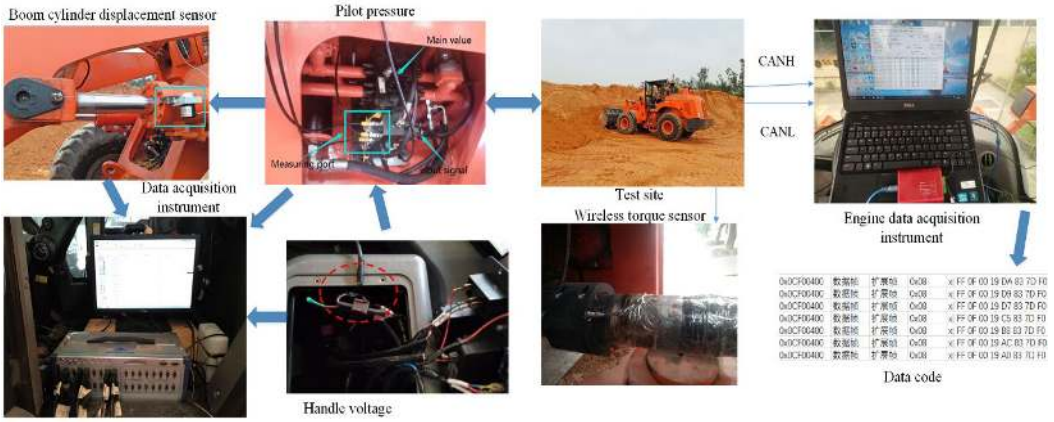

FIGURE 9. Shovel test equipment.

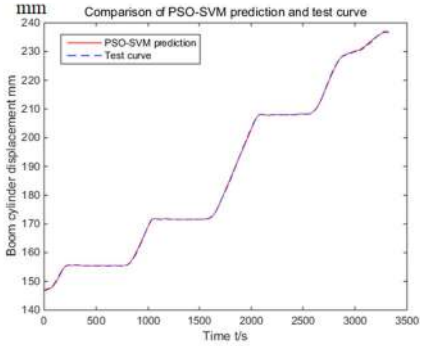

FIGURE 10. PSO-SVM regression prediction curve.

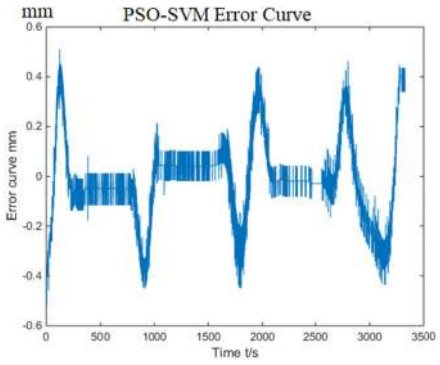

FIGURE 11. PSO-SVM regression prediction error curve.

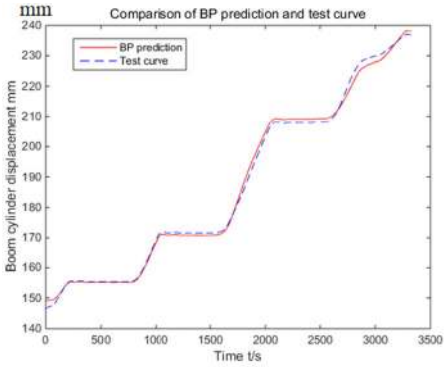

FIGURE 12. BP prediction curve.

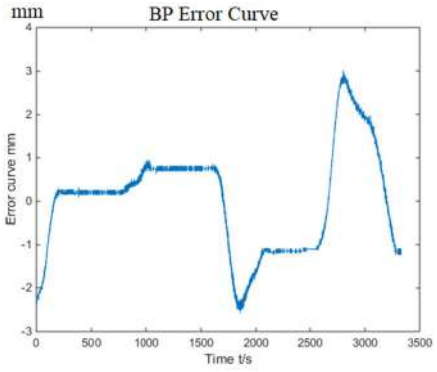

FIGURE 13. BP prediction error curve.

where:

$$\hat{H}(s) = \left(\frac{\omega_\mu}{\omega_h}\right)^{\alpha} \prod_{k=-N}^{N} \frac{1 + s/\omega_k'}{1 + s/\omega_k} \tag{20}$$

In the abovementioned equation:

$$\omega_k' = \omega_b \left(\frac{\omega_h}{\omega_b}\right)^{\frac{k+N+(1-\alpha)/2}{2N+1}} \tag{21}$$

$$\omega_k' = \omega_b \left(\frac{\omega_h}{\omega_b}\right)^{\frac{k+N+(1+\alpha)/2}{2N+1}} \tag{22}$$

According to equations (20), (21) and (22), the construction of the solver can be completed by building the Oustaloup filter in MATLAB/Simulink software platform, which is illustrated in Fig.15. Fig. 15(a) shows that the module encapsulation method of the Simulink software can be

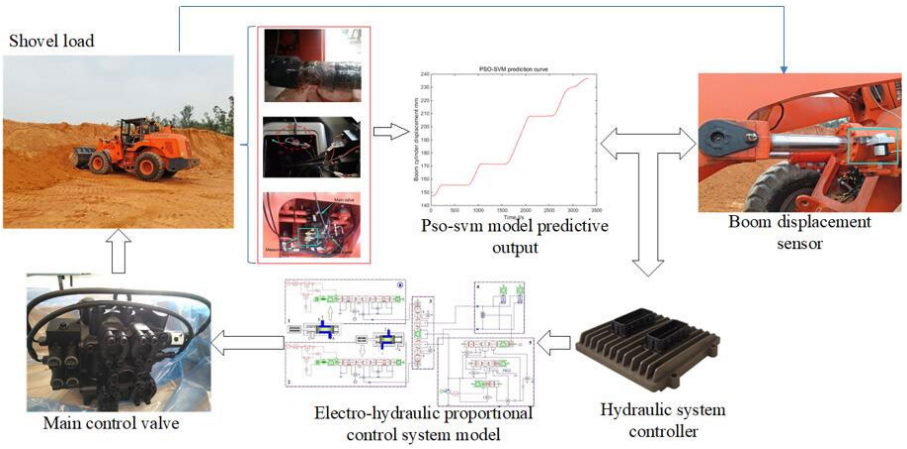

FIGURE 14. Skid-proof shovel loading process.

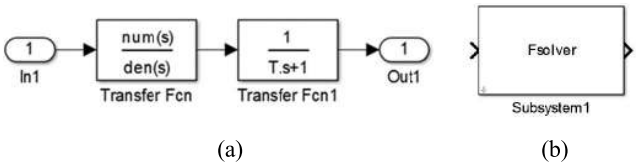

FIGURE 15. Structural block diagram and package diagram of the Oustaloup filter.

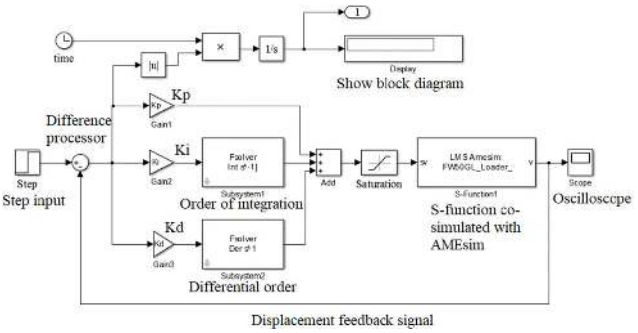

FIGURE 16. Fractional order PID control algorithm.

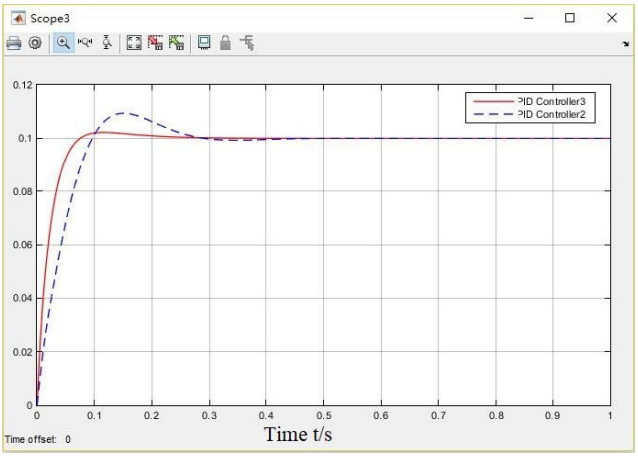

FIGURE 17. Step response of the fractional-order PID controller.

utilized to complete the encapsulation of the model. Moreover, Fig. 15(b) shows the fractional calculus solver.

Fig. 16 shows the simulink model of the fractional-order PID control algorithm. It should be indicated that the model is combined with the electro-hydraulic proportional control hydraulic system illustrated in Fig. 4 and the fractional-stage PID output current is sent to the electro-hydraulic proportional hydraulic system to control the movement of the boom cylinder. The displacement signal of the boom cylinder is regarded as the feedback to the simulink model of the fractional-order PID control algorithm.

Fig. 17 illustrates the step response of the controller. It is observed that the system step response using the fractional-order PID controller has a maximum overshoot of 2.5%, a settling time of 0.15 sand a rise time of 0.06 s, which meets design requirements.

The shovel test is carried out to verify the skid-proof control strategy of the wheel loader. Fig. 18 shows the obtained engine torque curve, the drive shaft torque curve and the electro-hydraulic proportional control hydraulic system pressure curve.

It can be seen from the test curve that the boom cylinder was lifted 4 times during the shovel test, and the engine torque and the transmission shaft strain were also reduced by 4 times. After the compact core is formed, when the wheel is about to slip, the transmission shaft strain and engine torque will decrease. The predictive model will raise the boom cylinder and destroy the compact core at this time, so that the transmission shaft strain and engine torque will increase. By repeatedly destroying the compact core like this, the engine torque can be rationally utilized and the tire slip can be reduced.

The shovel test curve indicates that the shovel loading operation starts from 36s and ends at 48s for a total time of 12s(Can be seen through the drive shaft torque curve).

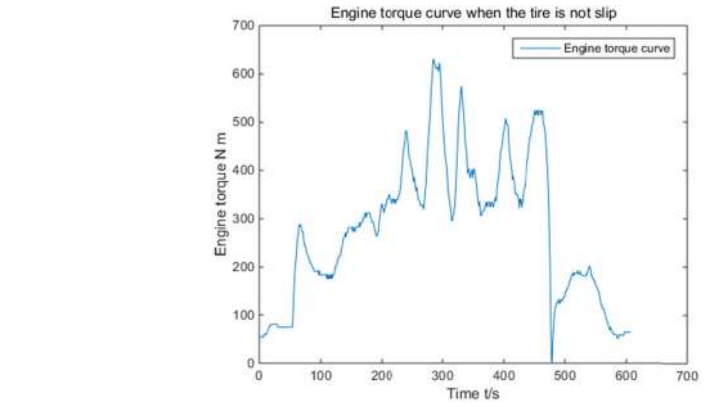

(a)

(b)

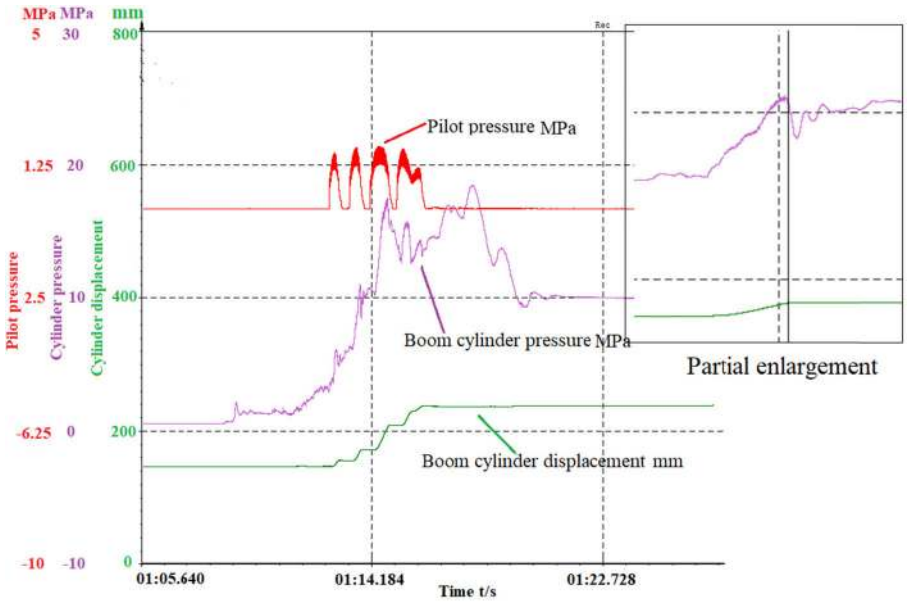

(c)

FIGURE 18. Shovel mounted skid-proof control strategy test.

When the wheel slip is about to occur, the hydraulic system controller generates a current to the electromagnetic proportional pressure reducing valve. Meanwhile, the displacement of the boom cylinder increases along the distance, which can damage the compact core. It is observed that both torques from the engine and the driveline are reduced. It is concluded

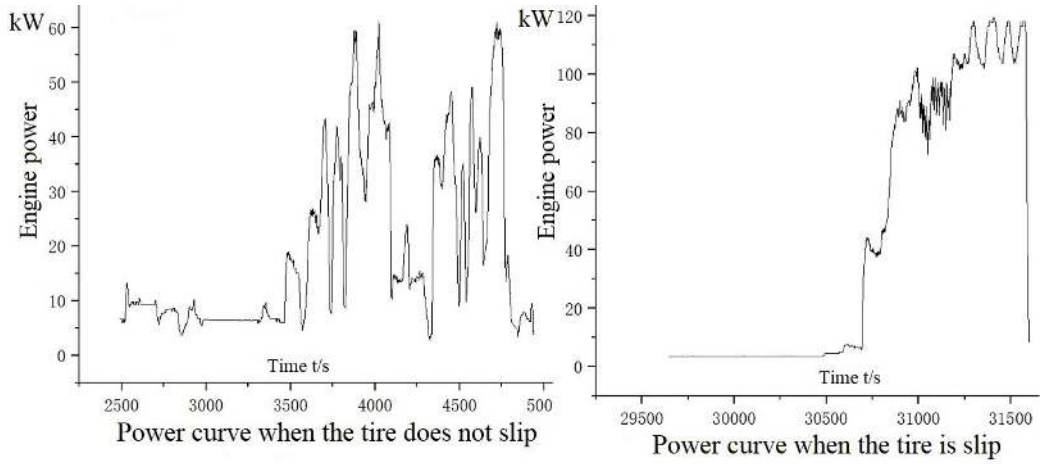

FIGURE 19. Comparison of power curves.

that when the slip is about to occur again, as the working depth increases, the boom raises continuously until the shoveling operation is over. Moreover, Fig. 19 shows that the engine power curve can be calculated from the torque and the engine speed (the left picture shows that the wheel does not slip, while the right picture shows the slipping wheel. According to the engine power curve, the skid-proof shoveling function designed in this paper can reduce the power loss. The test sites are all the same, and the working conditions are always the same.

VI. CONCLUSION

Large number of shovel tests proves that the tire causes a certain amount of power waste when it slips. In order to resolve this problem, the present study proposes a skid-proof strategy for the wheel loader working device. In the proposed scheme, the PSO-SVM regression prediction model is combined with the electro-hydraulic proportional control technology to control the on/off of the electromagnetic proportional pressure-reducing valve. As a result, the posture of the wheel loader working device is changed and the working resistance and the tire slippage are reduced.

The research content of the present study can be summarized as follows:

(1) The mechanism of the skid-proof shovel is analyzed theoretically. It is observed that the length of the compact core directly affects the insertion resistance. It is found that when the length of the compact core increases, the insertion resistance increases too. On the other hand, if the compact core is destroyed in time and its length is shortened, the insertion resistance reduces.

(2) The electro-hydraulic proportional control technology is introduced. Then it is applied to the wheel loader and the corresponding transfer function is obtained. The hydraulic simulation model of the electro-hydraulic proportional control is established by the AMEsim software, and then it is verified by experiments.

(3) The PSO algorithm is used to optimize SVM parameters. Moreover, the displacement of the boom cylinder is predicted and compared with the BP neural network prediction model. Through the analysis of prediction results, it is observed that the PSO-SVM prediction model of the boom cylinder displacement has reasonable generalization ability and high prediction accuracy.

(4) The skid-proof controller of the wheel loader is designed by the fractional-order PID control algorithm. The feasibility of the skid-proof control strategy is verified by the joint simulation with the electro-hydraulic proportional control hydraulic simulation model.

(5) The hydraulic system controller is prepared for the wheel loader shovel test. The test curve demonstrates the effectiveness of the skid-proof control strategy and the proposed algorithm.

The shortcomings of this paper are: (1) Controller overshoot is still a bit large. (2) The accuracy of the regression prediction model needs to be improved.

REFERENCES

[1] T. Muro, "Estimation of wear life of wheel loader tyre," *J. Terramechanicss*, vol. 29, no. 1, pp. 134–147, Nov. 1992.

[2] J. W. Shi, T. L. Lu, and X. W. Li, "Research on traction control of low attachment pavement of automatic transmission vehicles with automatic transmission," *J. Agricult. Mach.*, vol. 33, no. 2, pp. 127–132 and 147, Nov. 2011.

[3] Y. C. Wu, X. W. Ji, and P. Xie, "Four-wheel drive simulation analysis of ZL50 wheel loader based on active limited slip differential," *China Mech. Eng.*, vol. 22, no. 21, pp. 2638–2641, Jun. 2011.

[4] X. L. Zhang, R. Y. Sun, and H. Y. Ge, "ASR simulation research based on road surface dynamic recognition," *J. Hubei Automot. Ind. Inst.*, vol. 28, no. 4, pp. 1–4, Jun. 2014.

[5] J. H. Wang, Y. C. Wang, and T. J. Fu, "Structural analysis and performance evaluation of active controlled limited slip differential," *Automobile Technol.*, vol. 21, no. 7, pp. 35–43, Jul. 2008.

[6] A. Janulevi ius, G. Pupinis, and V. Kurkauskas, "How driving wheels of front-loaded tractor interact with the terrain depending on tire pressures," *J. Terramechanics*, vol. 12, no. 53, pp. 83–92, Nov. 2014.

[7] M. Duan, W. T. Guo, and G. Li, "Study on acceleration slip regulation control of electric based on road identification," *J. Mech. Electr. Eng.*, vol. 32, no. 9, pp. 132–1257 and1262, Aug. 2015.

[8] Y. F. Chen, Y. C. Wu, and X. X. Hu, "Four-wheel acceleration slip regulation of wheel loader based on pavement state identification," *J. Zhejiang Sci-Tech Univ.*, vol. 37, no. 5, pp. 681–686, Jun. 2017.
[9] S. Z. Fan, Y. D. Li, and J. Li, "Research on traction control of low-adhesive roads in automatic transmission vehicles," *J. Agricult. Mach.*, vol. 38, no. 8, pp. 127–132, Jun. 2007.
[10] H. X. Zheng, *Research on Automatic Anti-skid Differential System of Wheeled Construction Machinery*. Hunan, Changsha: Central South Forestry College 2003.
[11] Y. G. Yin, Y. S. Cheng, and J. M. Li, "Preliminary discussion on the soil of the wheel loader vibrating blade," *Construct. Mach. Equip.*, vol. 5, no. 6, pp. 25–29, Jan. 1989.
[12] D. Q. Fan, *The Experiment Research and Theoretical Analysis of Hydraulic Vibrating Loading on Wheel Wheel Loader*. Changchun, China: Jilin, 2006.
[13] M. G. Liu, S. G. Huang, and H. Su, "Engineering machinery electro-hydraulic proportional control technology and energy saving," *Construct. Mach. Technol. Manage.*, vol. 9, pp. 91–94, Jun. 2013.
[14] Y. You, L. P. Xu, and D. Z. Ren, "Design of electro-hydraulic proportional control system for excavators," *Mach. Tool Hydraulic*, vol. 40, no. 22, pp. 82–84, Aug. 2012.
[15] T. X. Gao, Q. Gao, and Y. Li, "Hydraulic leveling technology for electro-hydraulic proportional control based on fuzzy PID," *Appl. Mech. Mater.*, vol. 37, no. 5, pp. 503–510, Jun. 2014.
[16] R. Li, J. Luo, and C. G. Sun, "Analysis of electro-hydraulic proportional speed control system on conveyer," *Procedia Eng.*, vol. 31, pp. 1185–1193, Oct. 2012.
[17] M. L. Jiang, L. Jiang, and D. D. Jiang, "A sensor dynamic measurement error prediction model based on NAPSO-SVM," *Sensors*, vol. 18, pp. 233–238, Oct. 2018.
[18] C. X. Mu, R. M. Zhang, and C. Y. Sun, "Least squares support vector machine predictive control method for nonlinear systems based on particle swarm optimization," *Control Theory Appl.*, vol. 27, no. 2, pp. 164–168, Jun. 2010.
[19] J. J. Zhang, J. Y. Sun, and H. J. Chang, "Prediction of aircraft vibration environment based on support vector machines with particle swarm optimization algorithm," in *Proc. Int. Conf. Autom. Control Artif. Intell.*, vol. 37, Aug. 2012, pp. 1592–1595.
[20] I. D. Lins, M. das Chagas Moura, E. Zio, and E. L. Droguett, "A particle swarm-optimized support vector machine for reliability prediction," *Qual. Rel. Eng.*, vol. 28, pp. 141–158, Jun. 2012.
[21] D. C. Ceng, *Mechanical Soil Dynamics*. Beijing, China: Beijing Science and Technology Press, 1995.
[22] Y. G. Yin, J. M. Li, and G. Q. Wang, "Experimental study on two-dimensional vibration shovel," *J. Agricult. Mach.*, vol. 2, no. 25, pp. 18–23, Jun. 1994.
[23] Y. X. Wu, S. Y. Zhang, and Y. S. Huang, "Intelligent wheel loader drag reduction insertion shovel strategy," *Construct. Mach.*, vol. 10, pp. 25–31, Oct. 2003.
[24] H. Y. Ji, Y. F. Tan, and G. L. Jiang, "Soil surface change algorithm for bucket cutting," *Comput. Simul.*, vol. 1, pp. 105–111, Jan. 2004.
[25] C. Y. Zhao and J. X. Zhu, "Research on vibration excavation mechanism of hydraulic excavator," *Des. Res.*, vol. 11, pp. 125–131, Nov. 2005.
[26] J. X. Zhu, C. Y. Zhao, and X. F. Zou, "On-line identification of soil parameters for vibration excavation of hydraulic excavators," *J. Central South Univ.*, vol. 37, no. 3, pp. 537–541, Jun. 2006.
[27] Z. H. Li, J. T. Cao, and X. F. Ji, "Research on fault diagnosis of rolling bearing based on EEMD and CS-SVM," *Mech. Electr. Eng.*, vol. 19, no. 6, pp. 622–627, Jun. 2019.
[28] C. H. Zhao, H. X. Hu, and B. J. Chen, "Bearing fault diagnosis based on deep learning feature extraction and WOA-SVM state recognition," *Vib. Shock*, vol. 38, no. 10, pp. 31–48, Oct. 2019.
[29] Z. Zhang, X. Shao, and D. Yu, "Fault diagnosis of a wheel loader by artificial neural networks and fuzzy logic," in *Proc. IEEE Conf. Robot., Automat. Mechatronics*, Jun. 2006, pp. 1–5.
[30] M. Z. Lv, X. M. Su, and C. Z. Chen, "Application of improved particle swarm optimization algorithm for support vector machines in fault diagnosis of rolling bearings," *Mach. Electron.*, vol. 37, no. 1, pp. 42–48, Nov. 2019.
[31] Z. B. Shi, Q. G. Song, and M. Z. Ma, "Diagnosis for vibration fault of steam turbine based on modified particle swarm optimization support vector machine," *Appl. Mech. Mater.*, vol. 128, pp. 113–116, Jun. 2012.
[32] C. Y. Miao, Y. Q. Yang, and S. H. Han, "PID controller parameters optimization based on PSO," *Instrum. Anal. Monitor.*, vol. 4, pp. 1–3, May 2013.
[33] H. Zhengtong, G. Zhengqi, M. Xiaokui, and C. Wanglin, "Multimaterial layout optimization of truss structures via an improved particle swarm optimization algorithm," *Comput. Struct.*, vol. 222, pp. 10–24, Oct. 2019.
[34] W. Y. Ruan, Z. Q. Ma, and Y. C. Li, "Variational mode decomposition permutation entropy combined with particle swarm optimization support vector machine applying to rolling bearing fault diagnosis," *J. Univ. Jinan*, vol. 32, no. 4, pp. 291–296, Jun. 2018.

BINGWEI CAO received the master's degree from the Shandong University of Technology, Zibo, China, in 2016. He is currently pursuing the Ph.D. degree with Jilin University.

His current research interests include machine learning, image recognition, and hydraulics.

XINHUI LIU received the Ph.D. degree in applied mechanics from Jilin University, Jilin, China, in 1998. He is currently a Professor and a Doctoral Supervisor with the School of Mechanical and Aerospace Engineering, Jilin University. He is also the Executive Vice President of the Institute of Intelligent Manufacturing, Jilin University. His main research directions are fluid transmission and electro-hydraulic control, engineering machinery hydraulic transmission, engineering machinery electro-hydraulic control, engineering machinery hydraulic system energy-saving technology, engineering vehicle fluid composite drive technology, engineering vehicle electro-hydraulic combined simulation, hydraulic system test, data analysis and processing, and defense application technology.

WEI CHEN received the Ph.D. degree in mechatronic engineering from Jilin University, Jilin, China, in 2009.

He is currently an Associate Professor with the School of Mechanical and Aerospace Engineering, Jilin University. His research interests include mechanical and electrical engineering, and hydraulic and fluid transmission control.

KUO YANG is currently pursuing the master's degree with the School of Aerospace and Mechanical Engineering, Jilin University. His current research interests are machine learning and intelligent control.

PENG TAN is currently pursuing the Ph.D. degree with the School of Mechanical and Aerospace Engineering, Jilin University. His research interests are fluid transmission and electro-hydraulic control.